

Experimental investigation of the stability of the floating water bridge

Reza Montazeri Namin,¹ Ahmad Amjadi,² Shiva Azizpour Lindi,³ Nima Jafari,² and Peyman Irajizad²

¹*Department of Mechanical Engineering, Sharif University of Technology, Tehran, Iran.**

²*Medical Physics Laboratory, Department of Physics, Sharif University of Technology, Tehran, Iran.*

³*National Organization for Development of Exceptional Talents (NODET), Farzanegan Highschool, Tehran, Iran.*

(Dated: August 2, 2018)

When a high voltage is applied between two beakers filled with deionized water, a bridge of water may be formed in between exceeding the length of 2 cm when the beakers are pulled apart. We construct experiments in which the geometry and the electric field within the bridge are measured and compared with predictions of theories on the floating water bridge. A numerical simulation is used for the measurement of the electric field. Our experimental results approve that two forces of dielectric tension and surface tension are holding the bridge against gravity. These forces have the same order of magnitude. Results show that the stability can be explained by macroscopic forces, regardless of the microscopic changes in water structure.

PACS numbers:

I. INTRODUCTION

The floating water bridge is an interesting phenomenon first reported by Armstrong in 1893 [1]. After more than a century Fuchs et al [2] reported their investigation about this interesting phenomenon and showing the different behaviours in it, suggested that it could reveal some hidden properties of water [3]. Two beakers filled with deionized water are subjected to a DC high voltage more than 10kV and a bridge is formed between them (figure 1) which can last for hours and have a length exceeding 2cm [4]. This experiment is stable, easy to reproduce and leads to a special condition that the water in the bridge can be accessed and experimented under high voltages and different atmospheric conditions [5]. This has led to several special experiments in this setup, including Neutron scattering [6, 7], visualization using optical measurement techniques [3, 4], Raman scattering [8], Brillouin scattering [9] and zero gravity experiments [10], many of which have attempted to investigate the possible structural changes in the water bridge causing its formation, stability and other properties observed in the water bridge. Some observations have been explained by quantum electro dynamic theories [11]. Aqueous solutions have been tested under same setup and liquid bridging has been observed and conductivity and mass transfer differences have been investigated [12] as well as thermal differences in the behaviour of the bridge [13]. Also the bridging has been observed in liquids other than water [14]. Mid-infrared emission investigation of the water bridge suggest the existence of micro and nano droplets electro sprayed from the liquid-gas interface [15]. Transport and behaviour of bacterial cells added to the water bridge have also been investigated [16].

Reviews on this topic have been published [5, 17] which the reader may refer to for a comprehensive literature review.

While many discussions have been published regarding the structural changes in water leading to the stability of the bridge and suggest the existence of anisotropic chains of molecules in the bridge, high energy X-ray diffraction experiments show no preferred orientation of the molecules in the water bridge, which is also approved in molecular dynamics simulations [18]. In the present investigation, we concentrate on the theories based on macroscopic forces explaining the stability of the bridge. In this case there are two different perspectives: Widom et al in 2009 [19] suggest the existence of a tension along the bridge caused by the electric field within the dielectric material. They provide theoretical calculations based on the Maxwell pressure tensor within the dielectric to calculate this tension. The tension along the curved water bridge causes an upward force defying gravity. Marin and Lohse 2010 [14] apply a similar theory while the tension is calculated as half the value derived by [19], and in

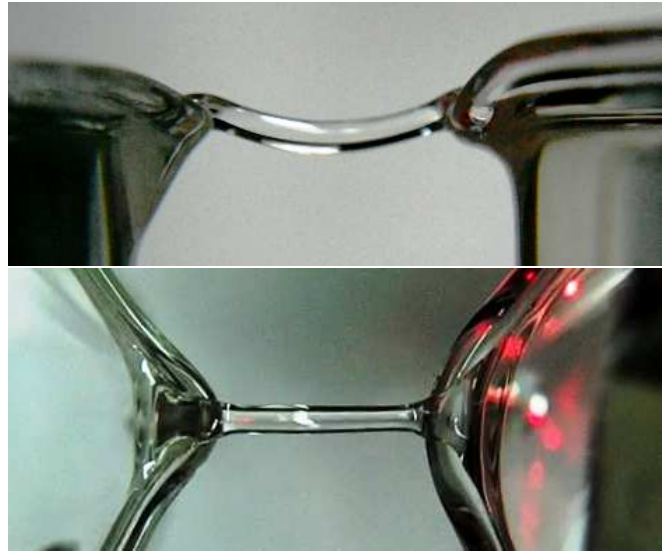


FIG. 1. The floating water bridge from Front and Top View

* namin@mech.sharif.edu; <http://mech.sharif.edu/~namin>

a modified experimental setup compare the results with experiments. They also measure water flow along the bridge suggesting electrical charges responsible for that. Morawetz 2012 [20, 21] discusses the effect of electrical charges in a charged catenary and solves the flow and derives stability criteria.

On the other hand, Aerov in 2011 [22] claims to prove that the tension caused by electric field within the dielectric material is zero and the only force holding the bridge against gravity is surface tension. The effect of the electric field according to Aerov is to avoid the breakup of the bridge into small droplets and maintain stability.

We try to examine the theoretical perspectives experimentally by designing quantitative experiments which are comparable with the two theories. The experimental setup is explained in section II. We precisely measure the geometry of the bridge by image processing, and estimate the electric field with use of a numerical simulation explained in part III. Experimental results and the theories are compared in section IV leading to conclusion.

II. EXPERIMENTS

The experimental setup consists of two 50ml beakers filled with deionized water. The water was produced with a Millipore SimPak1 purification pack kit and initially had a resistivity of 18.2 M Ω .cm. Resistivity of pure DI water decreases rapidly by contamination of impurities, e.g. the CO₂ gas from air. The resistivity in our experiments was reduced to 1.8 M Ω .cm. The resistivity also varies by temperature changes. It decreases from 1.8 M Ω .cm at 25°C to 1 M Ω .cm at 45°C.

A high voltage power supply was used which could provide a voltage upto 25 kV with 20 mA current intensity (Plastic Capacitors HV250-103M). A resistance of 50 M Ω was placed after the power supply as a ballast resistor to control the current in the circuit which had a great effect on the stability of the bridge, as shown in figure 2. Also a resistance of 100 Ω was placed so that the voltage difference along it demonstrates the current intensity. Two aluminium plates were placed at the far ends of the beakers in the water connected to the power supply. The voltage difference between the electrodes and the current intensity were measured. An infra-red thermometer (TES 1326S) was used to measure the surface temperature of water. The current intensity and experimenting time were kept small enough so that the temperature rise of the surface of water did not exceed 2°C and was kept between 24°C and 26°C during the experiments. So there might be about 5% of change of resistivity in different points in water.

Two cameras were recording the bridge from the top view and the front view. A third camera was recording the current intensity and voltage. For the extraction of quantitative data, we developed an image processing code using MATLAB to read the three movies and extract the desired data which includes the average diameter from

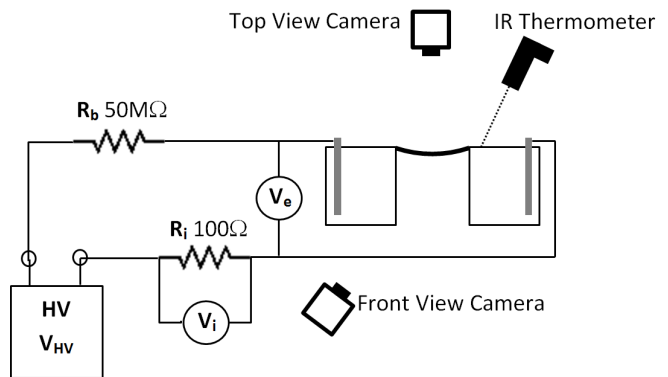


FIG. 2. Schematic of the experimental setup.

the top view D_t , the average diameter from the front view D_f , the curvature of the centreline of the bridge at its centre ξ , the voltage V and the current intensity I at every frame. To estimate the curvature of the centreline, initially the centreline was calculated by averaging the top and bottom of the bridge from the front view, then a parabola was fitted to the line and using the coefficient of the parabola the curvature was estimated. Also an error to this curvature was estimated by the regression of the fitted curve. The amount of voltage was used to estimate the electric field in the centre of the bridge as explained in section III.

III. EVALUATION OF THE ELECTRIC FIELD

To compare the shape of the bridge in experiments with the predictions of the theories, the precise value of the electric field was to be measured experimentally. For this propose we used a numerical simulation; the electric current (ec) module of the COMSOL Multiphysics program was used. The geometry of the bridge was approximately modelled and the average electric field was calculated at a cross section in the middle of the bridge (E).

In the simulation, water was assumed to be a conducting material with a constant resistivity and dielectric permittivity. The shape of the bridge and water in the beakers was carefully estimated by measuring the geometry of the beaker tips. During the experiments the beakers were filled with water to the top, so that the unknown geometry of the water connecting the water in the beaker to the water in the bridge becomes least important.

As a result of the simulation, it was observed that the electric field decreases with the increase of diameter of the bridge. Also defining $E^* = V/l$, the ratio E/E^* increases and approaches to one with the increase of the bridge length. This ratio seems to be only a function of l/D , and not a function of l and D independently. According to figure 4 b), there is a linear relation between E^*/E and D/l . The effect of curvature on the electric field was less

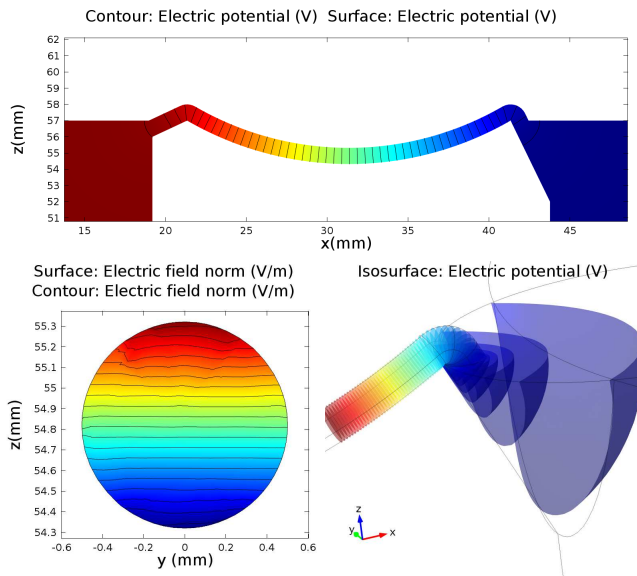


FIG. 3. Results of the Numerical Simulation. a) Contours of Electric Potential on a Cut Plane at $y = 0$. It shows that the equipotential surfaces are oriented normal to the bridge centreline. b) Contours of Electric Field Intensity on a Cross-Section at the Middle of the Bridge. The upward gradient of the electric field is the cause of the dielectric force holding the bridge. Calculations regarding this factor are presented in section IV and Appendix. c) Equipotential Surfaces Near the Tip of One Beaker.

than 1.5% in the range of experiments and was neglected. Also an estimation on the uncertain geometric properties was performed, such as the elevation difference of the water in the beaker (which in experiments was less than 0.5mm), and as a result errors caused by this geometric approximations was less than 8% for $l = 10\text{mm}$ and less than 5% for $l = 20\text{mm}$. This was the most important factor in determining the error bars.

IV. RESULTS AND DISCUSSION

The extracted data from experiments are the average diameter from top view D_t , average diameter from front view D_f , curvature of the bridge from the front view ξ , voltage difference between the electrodes V_e and current intensity I . Every five extracted data (0.2s) has been averaged to present one data point. The distance between the beaker tips l_b and the voltage difference across the high voltage supply V_{HV} were the independent parameters we could change during experiments. Our experimental data is presented in figure 5.

Figure 5 shows that by increasing the voltage produced by the power supply, the voltage difference between the electrodes does not change significantly. Instead, current intensity increases and the residual voltage will be dropped at the ballast resistor. The reason for this fact seems to be that the diameter of the bridge increases with

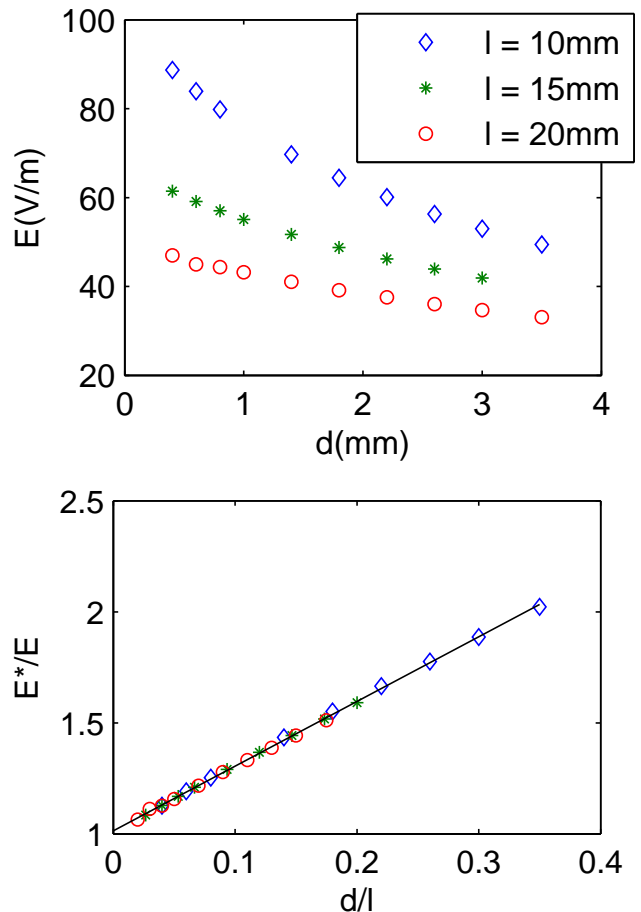


FIG. 4. a) Evaluated Electric Field From the Numerical Simulation. $V = 1\text{V}$, $\xi = 0.001$, for three values of l . b) Analysed Data. The line represents a linear fit: $E^*/E = 2.9096(D/l) + 1.0144$ with the Regression of $R^2 = 0.98$.

the increase of current intensity, causing a fairly linear relation between current intensity and cross-sectional area of the bridge. This causes the electric resistance of the bridge to drop with an increase in current intensity and as a result the voltage drop across the bridge remains fairly constant. In the absence of the ballast resistor, the water in the beaker acts fairly similar to the ballast resistor keeping the voltage difference across the bridge constant in different current intensities. We suggest this to be a reason for not achieving longer bridges in higher electric voltages; i.e. by increasing the electric voltage, bridge increases its thickness passing a higher current intensity and the electric field along the bridge remains constant and does not increase.

To analyse the experimental data, the average diameter of the bridge was calculated as $D = \sqrt{D_t D_f}$ and the electric field was estimated using the results of section III as a function of V_e and D and the length of the bridge l .

To quantitatively compare our experiments with theoretical results of Widom et al [19] and Aerov [22], their theory is used to find the fraction of their suggested forces

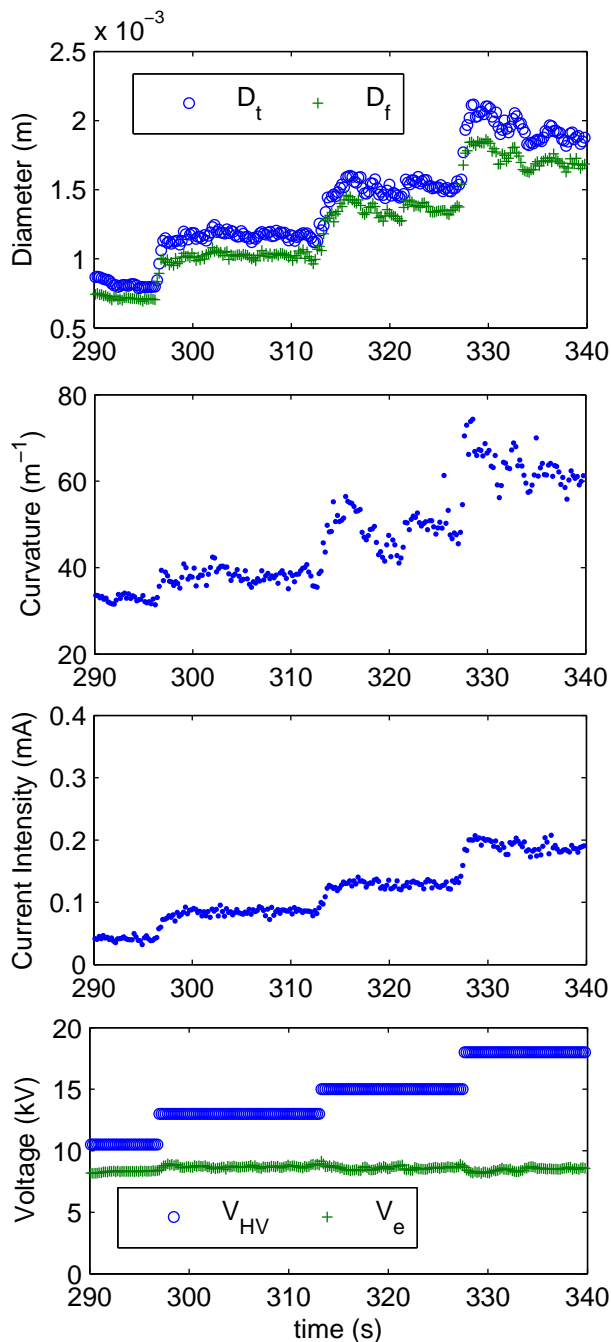


FIG. 5. Data extracted directly from experiments in means of time. a) Diameters from top and side view b) Curvature of the bridge centreline c) Current intensity passing through the bridge. d) Voltage differences across the electrodes (V_e) and the power supply (V_{HV}). Time is started with the bridge formation.

to the force needed to hold the bridge in experiments. In the equilibrium condition, since the sum of the vertical forces holding the bridge should be zero, the total fraction of the holding forces to the gravitational force must be equal to one.

The tension because of the electric field in a dielec-

tric medium calculated by Widom et al [19] follows this relation:

$$T_{DE} = \varepsilon_0(\varepsilon - 1)E^2A. \quad (1)$$

Where A is the cross sectional area of the bridge, and is equal to $\pi D^2/4$, ε is the relative permittivity of the water, which was assumed to be 80 and ε_0 is the vacuum permittivity. If a tension T is acting on a curved bridge with a curvature of ξ , the vertical force it causes per unit length of the bridge is ξT , while the gravitational force per unit length is $\rho A g$. Thus the ratio of the dielectric force and gravitational force (R_{DE}) will be:

$$R_{DE} = \frac{\varepsilon_0(\varepsilon - 1)E^2\xi}{\rho g}. \quad (2)$$

We have also calculated the upward force exerted by the electric field in a curved dielectric bridge with a different method from Widom et al [19] which leads to the same force as they have calculated; explained in Appendix.

Aerov [22] states that the electric tension along the bridge is zero, and the tension holding the bridge is the surface tension. The electric field causes the stability of the bridge and avoids its breakup to droplets. The tension caused by surface tension is the sum of the tension on the sides (γP) and the repulsing tension caused by pressure jump at the surface ($-\gamma P/2$):

$$T_{ST} = \frac{1}{2}\gamma P. \quad (3)$$

where P is the perimeter of the cross-section of the bridge and is equal to πD . According to this assumption, the ratio between the upwards surface tension force and gravitational force (R_{ST}) can be calculated as:

$$R_{ST} = \frac{2\gamma\xi}{\rho g D}. \quad (4)$$

We have calculated R_{DE} and R_{ST} and also the sum of the two fractions for our experimental data as plotted in figure 6. The results suggest that the sum of the dielectric force as calculated by Widom et al [19] and the surface tension force as calculated by Aerov [22] are sufficient for the vertical equilibrium of the bridge. Also the two forces have the same order of magnitude, both being important and neither of the forces are negligible.

V. CONCLUSION

We have experimentally investigated the forces holding the floating water bridge against gravity. By analysing the shape of the bridge from top and side views and evaluating the electric field using a numerical simulation, we have estimated the forces of dielectric tension and surface tension and compared them to the weight of the bridge.

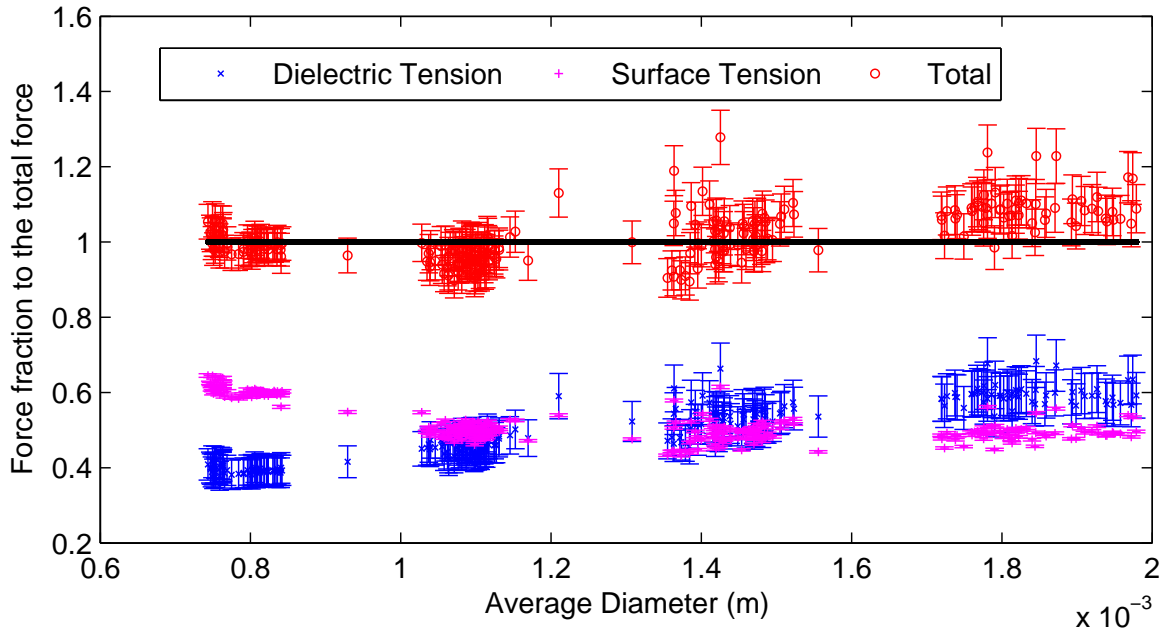


FIG. 6. Ratio of the calculated forces to the force needed to hold the bridge. This result suggests that a sum of the surface tension and dielectric tension are convenient to explain the vertical equilibrium of the bridge. $l = 14mm$.

Our results show that the vertical components of the two forces of dielectric tension in water and surface tension hold the bridge against gravity. Our data shows that in smaller diameters of the bridge the effect of surface tension gets more important, while in thick bridges the dielectric tension is more important in holding the bridge. Our data shows that neither of the two forces are negligible, each being responsible for about half of the weight of the bridge and the sum of them is equal to the weight of the bridge.

We have shown that increasing the electric voltage of the power supply does not necessarily increase the electric field along the bridge, because the cross-sectional area of the bridge varies fairly linear with current intensity. We suggest this to be a reason for not achieving bridges longer than $2.5mm$ in high electric voltages in experiments, and also an explanation for Aerov's claim [22] about the dielectric tension hypothesis: "The electrostatic field hypothesis of the bridge tension ($\tau \sim E^2$) is not really consistent with experiments, because it allows the existence of bridges longer than 4 cm in stronger fields, which seems to be not the case."

We have shown that the stability of the floating water bridge can be fully explained with the two forces of dielectric tension and surface tension. Changes in the structure of water are not needed for explaining the stability.

ACKNOWLEDGMENTS

We wish to thank Prof. K. Morawetz and Prof. A. Aerov for helpful discussions in different stages of our investigation. We acknowledge the International Young Physicists' Tournament (IYPT) society for introducing this phenomenon and for discussions at IYPT 2012 Bad Saulgau Germany. We also thank Sharif Applied Physics Research Center for its financial support at Medical Laser Physics Lab.

Appendix: Upward Dielectric Force in the Water Bridge

We directly calculate the vertical force exerted to the dielectric according to the vertical gradients of the electric field. Note that equipotential surfaces along the bridge must be normal to the surface of the bridge since no electric current can flow normal to the surface. Thus equipotential surfaces are approximately normal to the bridge centreline. This assumption is verified in numerical simulations as shown in figure.3 a). As a result, equipotential surfaces are closer at the top of the bridge and far at the bottom, so a higher electric field exists at the top. This causes an upward body force to the bridge as:

$$F_b = \frac{1}{2}\epsilon\nabla E^2. \quad (\text{A.1})$$

Assuming the equipotential surfaces to be flat and normal to the bridge centreline (as shown in Fig. 3 a), the electric

field in the centre of the water bridge is totally in the direction of the length of the bridge and can be calculated as a function of elevation z :

$$E(z) = E_m \frac{1}{1 - z\xi}. \quad (\text{A.2})$$

Where E_m is the electric field at the altitude of zero which is the centreline of the bridge. Thus at the centre

of the bridge:

$$\frac{\partial E^2}{\partial z} = 2E_m^2 \xi F_b = \epsilon E^2 \xi. \quad (\text{A.3})$$

This body force must equal to the gravitational body force in case of equilibrium, thus:

$$\epsilon E^2 \xi = \rho g \Rightarrow \xi = \frac{\rho g}{\epsilon E^2}. \quad (\text{A.4})$$

Which is the same as equation 2 derived from the theory of Widom et al [19]. This might be a reason showing the existence and correctness of the dielectric tension calculated therein.

-
- [1] W. Armstrong, *The Electrical Engineer* **10**, 153 (1893).
 - [2] E. Fuchs, J. Woisetschläger, K. Gatterer, E. Maier, R. Pecnik, G. Holler, and H. Eisenkölbl, *Journal of Physics D: Applied Physics* **40**, 6112 (2007).
 - [3] E. Fuchs, K. Gatterer, G. Holler, and J. Woisetschläger, *Journal of Physics D: Applied Physics* **41**, 185502 (2008).
 - [4] J. Woisetschläger, K. Gatterer, and E. Fuchs, *Experiments in fluids* **48**, 121 (2010).
 - [5] E. Fuchs, *Water* **2**, 381 (2010).
 - [6] E. Fuchs, B. Bitschnau, J. Woisetschläger, E. Maier, B. Beuneu, and J. Teixeira, *Journal of Physics D: Applied Physics* **42**, 065502 (2009).
 - [7] E. Fuchs, P. Baroni, B. Bitschnau, and L. Noirez, *Journal of Physics D: Applied Physics* **43**, 105502 (2010).
 - [8] R. Ponterio, M. Pochylski, F. Aliotta, C. Vasi, M. Fontanella, and F. Saija, *Journal of Physics D: Applied Physics* **43**, 175405 (2010).
 - [9] E. Fuchs, B. Bitschnau, S. Di Fonzo, A. Gessini, J. Woisetschläger, and F. Bencivenga, (2009).
 - [10] E. Fuchs, L. Agostinho, A. Wexler, R. Wagterveld, J. Tuinstra, and J. Woisetschläger, *Journal of Physics D: Applied Physics* **44**, 025501 (2010).
 - [11] E. Del Giudice, E. Fuchs, and G. Vitiello, arXiv preprint arXiv:1004.0879 (2010).
 - [12] M. Eisenhut, X. Guo, A. Paulitsch-Fuchs, and E. Fuchs, *Central European Journal of Chemistry* **9**, 391 (2011).
 - [13] E. Fuchs, A. Wexler, L. Agostinho, M. Ramek, and J. Woisetschläger, in *Journal of Physics: Conference Series*, Vol. 329 (IOP Publishing, 2011) p. 012003.
 - [14] Á. G. Marín and D. Lohse, *Physics of Fluids* **22**, 122104 (2010).
 - [15] E. Fuchs, A. Cherukupally, A. Paulitsch-Fuchs, L. Agostinho, A. Wexler, J. Woisetschläger, and F. Freund, *Journal of Physics D: Applied Physics* **45**, 475401 (2012).
 - [16] A. Paulitsch-Fuchs, E. Fuchs, A. Wexler, F. Freund, L. Rothschild, A. Cherukupally, and G. Euverink, *Physical Biology* **9**, 026006 (2012).
 - [17] J. Woisetschläger, A. Wexler, G. Holler, M. Eisenhut, K. Gatterer, and E. Fuchs, *Experiments in fluids*, 1 (2012).
 - [18] L. Skinner, C. Benmore, B. Shyam, J. Weber, and J. Parise, *Proceedings of the National Academy of Sciences* (2012).
 - [19] A. Widom, J. Swain, J. Silverberg, S. Sivasubramanian, and Y. Srivastava, *Physical Review E* **80**, 016301 (2009).
 - [20] K. Morawetz, *Physical Review E* **86**, 026302 (2012).
 - [21] K. Morawetz, *AIP Advances* **2**, 022146 (2012).
 - [22] A. Aerov, *Physical Review E* **84**, 036314 (2011).